J Therm Anal Calorim (2011) 106:165–172
DOI 10.1007/s10973-011-1582-x

Thermokinetic parameters and thermal hazard evaluation for three organic peroxides by DSC and TAM III

Shang-Hao Liu · Chun-Ping Lin · Chi-Min Shu

NATAS2010 Conference Special Issue

Abstract The thermokinetic parameters were investigated for cumene hydroperoxide (CHP), di-tert-butyl peroxide (DTBP), and tert-butyl peroxybenzoate (TBPB) by non-isothermal kinetic model and isothermal kinetic model by differential scanning calorimetry (DSC) and thermal activity monitor III (TAM III), respectively. The objective was to investigate the activation energy (E_a) of CHP, DTBP, and TBPB applied non-isothermal well-known kinetic equation to evaluate the thermokinetic parameters by DSC. We employed TAM III to assess the thermokinetic parameters of three liquid organic peroxides, obtained thermal runaway data, and then used the Arrhenius plot to obtain the E_a of liquid organic peroxides at various isothermal temperatures. In contrast, the results of non-isothermal kinetic algorithm and isothermal kinetic algorithm were acquired from a highly accurate procedure for receiving information on thermal decomposition characteristics and reaction hazard.

S.-H. Liu · C.-M. Shu (✉)
Department of Safety, Health, and Environmental Engineering, National Yunlin University of Science and Technology (NYUST), 123, University Rd., Sec. 3, Douliou, Yunlin 64002, Taiwan, ROC
e-mail: shucm@yuntech.edu.tw

C.-P. Lin
Department of Health and Nutrition Biotechnology, College of Health Science, Asia University, 500, Lioufeng Rd., Wufeng, Taichung 41354, Taiwan, ROC

Keywords Differential scanning calorimetry · Liquid organic peroxides · Reaction hazard · Thermal activity monitor III · Thermokinetic parameters

List of symbols

A	Pre-exponential factor (s^{-1})
C_A	Sample concentration (mol L^{-1})
C_p	Heat capacity (J g^{-1} K^{-1})
E_a	Activation energy (kJ mol^{-1})
$f(\alpha)$	Kinetic functions
k	Reaction rate constant (min^{-1})
k_i	Reaction rate constant at isothermal temperature (min^{-1}, $i = 0, 1, 2, 3$)
k_{iso}	Rate constant at isothermal temperature (min^{-1}, ISO = 80, 90, 100, 110, 120)
M	Molecular weight (g mol^{-1})
m	Sample mass (g)
n	Reaction order (dimensionless)
Q	Heat of decomposition at time t (W g^{-1})
Q_0	Total heat of decomposition (kJ kg^{-1})
Q_t	Decomposition heat released at time t (kJ kg^{-1})
R	Gas constant (8.31415 J K^{-1} mol^{-1})
r	Reaction rate (g s^{-1})
T_0	Exothermic onset temperature (°C)
T_f	Final temperature (°C)
T_i	Peak temperature of different scanning rates (°C, $i = P_1, P_2, P_3$)
T_j	Different isothermal temperatures (°C, $j = 0, 1, 2, 3$)
TCL	Time to conversion limit (day)
TMR_{iso}	Time to maximum rate under isothermal conditions (min)
T_P	Peak temperature (°C)
t	Time (s)

α	Conversion rate (dimensionless)
β_i	Scanning rate (°C min^{-1}, i = 1, 2, 4, 10)

Introduction

The chemical characteristics of liquid organic peroxides are complex, sophisticated, and difficult to forecast, and have not been investigated completely in recent years. Thus far, there have been numerous explosive accidents of runaway reaction with organic peroxides in chemical industries. The exothermic quantity and gaseous pollution for thermal decomposition of organic peroxides are so enormous that could inevitably become a thermal hazard in chemical processes.

Cumene hydroperoxide (CHP) is produced by the oxidation of cumene with air and as a catalyst in the process of aqueous sodium carbonate. In industry, there are over 94.5% of the CHP employed in producing phenol and acetone by means of catalytic reaction [1]. In addition, CHP is as an initiator for polymerization that is used to yield the acrylonitrile–butadiene–styrene (ABS) resin [2].

In general, di-tert-butyl peroxide (DTBP) is a strong source of radicals in that the theoretical active oxygen content is 10.9 mass%. DTBP acts as a crosslinking agent applied in industry widely. DTBP is as an initiator for monomer polymerization, and polypropylene modifier, and is also used in the paint industry [3].

Tert-butyl peroxybenzoate (TBPB) is a strong free radical source containing more than 8.1 mass% of active oxygen. It is used as a polymerization initiator, catalyst, and vulcanizing agent, cross-linking agent, and as a chemical intermediate. TBPB is most widely applied in the polymerization of styrene, acrylates, methacrylates, ethylene, and in cross-linking peroxides, etc. TBPB can be used for polymerization and copolymerization for styrene in the temperature range of 100–140 °C. In other manufacturing processes, the temperature is significantly higher. The half-life temperature is 100 °C for 10 h [4].

CHP, DTBP, and TBPB are three unstable reactive chemicals owing to their weak oxygen–oxygen bond [2, 3, 5]. Their decomposition involves quickly heating and suddenly exposing influence of light, followed by potential fire and explosion hazards. When the organic peroxides are reacted with incompatible substances or ignition sources (acids, bases, reducing agents, and specific metals) [6], a runaway reaction will be created. They should be stored in a dry and refrigerated (<30 °C recommended or 38 °C max) area and should be kept away from reducing agents and incompatible substances. CHP, DTBP, and TBPB are given a hazard classification as a reactivity type by the National Fire Protection Association (NFPA) [7].

We investigated the thermokinetic parameters for CHP, DTBP, and TBPB by differential scanning calorimetry (DSC) [8]. The activation energy (E_a) for CHP, DTBP, and TBPB at different scanning rates (1, 1.5, 2, and 2.5 °C min^{-1}) were tested by DSC. Accordingly, we employed DSC thermal analysis to determine CHP, DTBP, and TBPB for the thermokinetic parameters of thermal decomposition. Furthermore, the aim was to evaluate thermal experimental data of CHP, DTBP, and TBPB via DSC, by applying the Ozawa kinetic equation [9–11] at various scanning rates. This was done along with a comparison of the mathematical approaches to build up the thermal decomposition properties for these three liquid organic peroxides.

Moreover, the microcalorimeter, thermal activity monitor III (TAM III), was applied to detect and record the exothermic activity of CHP, DTBP, and TBPB under isothermal conditions at the temperature range of 80–110 °C [12]. Under isothermal conditions, adiabatic calorimeters and conventional calorimeters, such as the vent sizing package 2 (VSP2) and DSC, respectively, are unable to detect the extremely weak heat-release of CHP, DTBP, and TBPB [13–18]. The aim of this research was to prove the thermokinetic decomposition properties and to establish a simplified isothermal kinetic model to illustrate the exothermic decomposition of CHP, DTBP, and TBPB by using an isothermal microcalorimeter to obtain the required data. By TAM III, the obtained thermal runaway data, such as heat flow (Q), reaction rate constant (k_{iso}), and time to maximum rate (TMR_{iso}) can be fully exploited for thermal hazard evaluation and emergency planning, as well as for designing an emergency relief system with the methodology of Design Institute for Emergency Relief Systems (DIERS) sponsored by the American Institute of Chemical Engineers (AIChE) [19].

Experimental and methods

Samples

DTBP of 98 mass%, a limpid liquid, was purchased from ALDRICH. CHP of 80 mass% and TBPB of 98 mass%, two light yellow liquid, were purchased from Alfa Aesar and ALDRICH, respectively. They were stored in a refrigerator at 4 °C. Experimental techniques, such as preliminary estimate, DSC, and TAM III were proposed earlier [20].

Differential scanning calorimetry (DSC)

Dynamic scanning experiments were performed on a Mettler TA8000 system coupled with a DSC 821^e measuring test crucible (Mettler ME-26732), that is the essential part of the experiment; it was used for carrying out the experiments for withstanding relatively high pressure to approximately 100 bar. STAR^e software was used to obtain thermal curves [8, 21]. The scanning rates selected for the temperature-programmed ramp were 1, 1.5, 2, and 2.5 °C min^{-1}. The range of temperature rise was chosen from 30 to 300 °C for CHP, DTBP, and TBPB. About 2–3 mg of the sample was used for acquiring the experimental data. The test cell was sealed manually by a special tool equipped with Mettler's DSC.

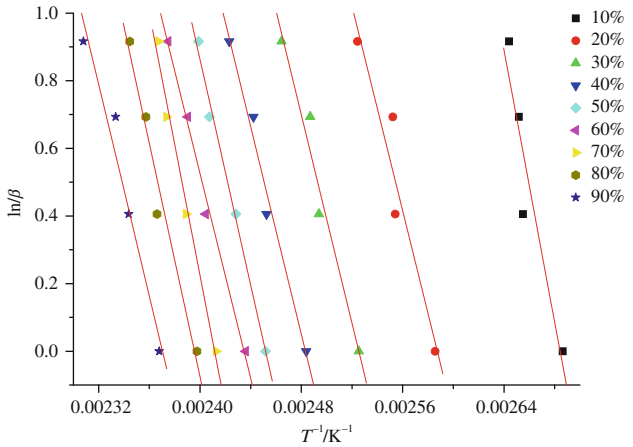

Fig. 1 Activation energy analysis graphs for CHP at scanning rates of 1, 1.5, 2, and 2.5 °C min^{-1} under α at 10, 20, 30, 40, 50, 60, 70, 80, and 90% by Ozawa-Flynn-Wall kinetic equation

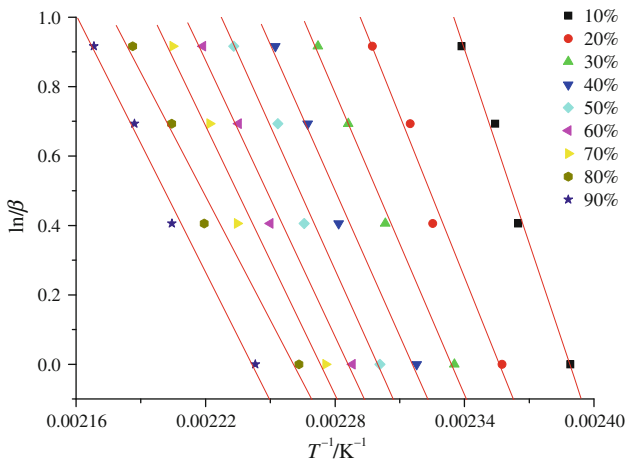

Fig. 2 Activation energy analysis graphs for DTBP at scanning rates of 1, 1.5, 2, and 2.5 °C min^{-1} under α at 10, 20, 30, 40, 50, 60, 70, 80, and 90% by Ozawa-Flynn-Wall kinetic equation

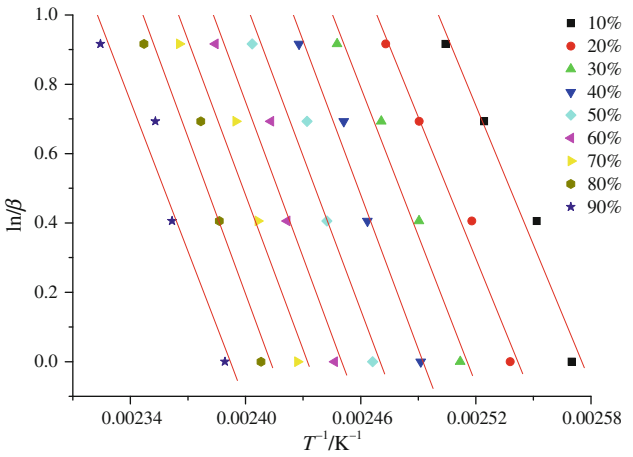

Fig. 3 Activation energy analysis graphs for TBPB at scanning rates of 1, 1.5, 2, and 2.5 °C min^{-1} under α at 10, 20, 30, 40, 50, 60, 70, 80, and 90% by Ozawa-Flynn-Wall kinetic equation

Table 1 CHP's thermokinetic parameters for the thermal decompositions in various degrees of conversion 10, 20, 30, 40, 50, 60, 70, 80, and 90% by Ozawa-Flynn-Wall kinetic equation

α/%	E_a/ kJ mol^{-1}	Correlation coefficient, R^2	Standard deviation, SD
10	159.18	0.899	0.151
20	119.90	0.920	0.137
30	121.86	0.964	0.093
40	121.64	0.982	0.066
50	131.87	0.993	0.041
60	119.89	0.992	0.043
70	153.33	0.986	0.057
80	136.49	0.970	0.084
90	123.67	0.961	0.096
Average	131.98	97.2[a], 107.7[b]	Decomposition mechanism/ autocatalytic[a]

[a] Li and Koseki [23]

[b] The E_a value was via Arrhenius plot by TAM III tests

Thermal activity monitor III (TAM III)

TAM III was applied to investigate the runaway reaction under temperatures of 80, 90, 100, and 110 °C [12]. Absolute temperature could be adjusted to within 0.02 K; while operating in isothermal mode, the bath mean temperature fluctuations were within 10^{-5} K. A maximum scanning rate was ± 2 K h^{-1} for chemical and physical equilibrium. We used the software of TAM III assistant to govern the thermostat. The thermostat liquid is mineral oil with a total volume of 22 L, and the temperature range of the thermostat is 15–150 °C when mineral oil is employed [12, 22].

Table 2 DTBP's thermokinetic parameters for the thermal decompositions in various degrees of conversion 10, 20, 30, 40, 50, 60, 70, 80, and 90% by Ozawa-Flynn-Wall kinetic equation

α/%	E_a/kJ mol^{-1}	Correlation coefficient, R^2	Standard deviation, SD
10	147.10	0.991	0.047
20	122.70	0.982	0.065
30	114.58	0.995	0.034
40	110.59	0.985	0.060
50	109.15	0.984	0.061
60	104.81	0.985	0.059
70	102.19	0.975	0.076
80	94.01	0.979	0.070
90	97.70	0.992	0.043
Average	111.43	78.3[a], 117[b]	Decomposition mechanism/ n-th order[a]

[a] Li and Koseki [23]

[b] The E_a value was via Arrhenius plot by TAM III tests

Table 3 TBPB's thermokinetic parameters for the thermal decompositions in various degrees of conversion 10, 20, 30, 40, 50, 60, 70, 80, and 90% by Ozawa-Flynn-Wall kinetic equation

α/%	E_a/kJ mol^{-1}	Correlation coefficient, R^2	Standard deviation, SD
10	105.78	0.899	0.154
20	107.61	0.920	0.137
30	112.87	0.964	0.093
40	117.04	0.982	0.066
50	116.92	0.993	0.040
60	118.18	0.992	0.043
70	117.59	0.986	0.057
80	119.11	0.970	0.084
90	114.13	0.961	0.096
Average	114.36	109[a], 115.8[b]	Decomposition mechanism/ n-th order[a]

[a] Lin et al. [24]

[b] The E_a value was via Arrhenius plot by TAM III tests

Results and discussion

Non-isothermal kinetic algorithm

Determination of thermokinetic parameters by Ozawa equation

Formal models can be represented on the basis of scanning rate that may consist of several dependent equations as illustrated by the following patterns [9–11].

Table 4 Results of experimental data for CHP's thermal decomposition via STAR^e software by DSC tests

β/°C min^{-1}	Integral/mJ mg^{-1}	T_0/°C	T_P/°C	T_f/°C
1	3892.31	123.78	140.20	150.54
1.5	3239.59	127.28	146.19	158.04
2	3815.28	130.35	148.98	160.81
2.5	3322.77	135.89	149.69	156.99

Table 5 Results of experimental data for DTBP's thermal decomposition via STAR^e software by DSC tests

β/°C min^{-1}	Integral/mJ mg^{-1}	T_0/°C	T_P/°C	T_f/°C
1	1648.40	120.34	163.71	188.56
1.5	2074.89	132.33	171.41	203.81
2	2274.82	148.64	174.70	192.26
2.5	2080.34	150.38	178.55	196.54

Table 6 Results of experimental data for TBPB's thermal decomposition via STAR^e software by DSC tests

β/°C min^{-1}	Integral/mJ mg^{-1}	T_0/°C	T_P/°C	T_f/°C
1	3515.85	81.22	136.74	154.52
1.5	3035.16	81.49	140.87	160.88
2	3180.62	117.28	139.17	161.37
2.5	2683.50	118.47	146.15	165.16

$$\ln(\beta) = -1.0516\frac{E_a}{RT_P} + \text{ const.} \quad (1)$$

At different scanning rates, a set of kinetic equations can be derived [9–11]:

$$\ln\beta_1 + 1.0516\frac{E_a}{RT_{P_1}} = \ln\beta_2 + 1.0516\frac{E_a}{RT_{P_2}} = \ln\beta_3 + 1.0516\frac{E_a}{RT_{P_3}} = \ldots \quad (2)$$

The activation energy analysis graphs for CHP, DTBP, and TBPB with different scanning rates of 1, 1.5, 2, and 2.5 °C min^{-1} by kinetic equation are illustrated in Figs. 1, 2, and 3. From Tables 1, 2, and 3, the E_a computed by the kinetic equation were 131.98, 111.43, and 114.36 kJ mol^{-1}, and the correlation coefficients were 0.963, 0.985, and 0.963 for the three organic peroxides.

Curve fitting approach and well-known kinetic equations were based on model fitting and model free method, respectively. In fact, we should be concerned with the accuracy problem for the curve fitting approach. From Tables 4, 5, and 6, we clearly observed greater scanning of more than 2.5 °C min^{-1}, the lesser than stability of thermal decomposition phenomenon is demonstrated for the kinetic

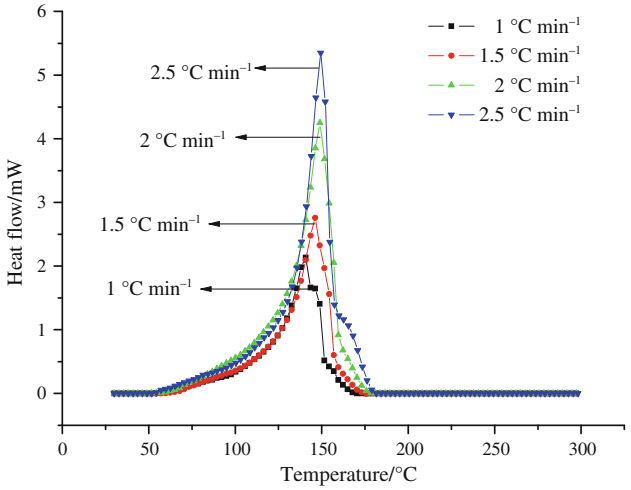

Fig. 4 DSC thermal curves of heat flow versus temperature for CHP decomposition with scanning rates of 1, 1.5, 2, and 2.5 °C min^{-1}

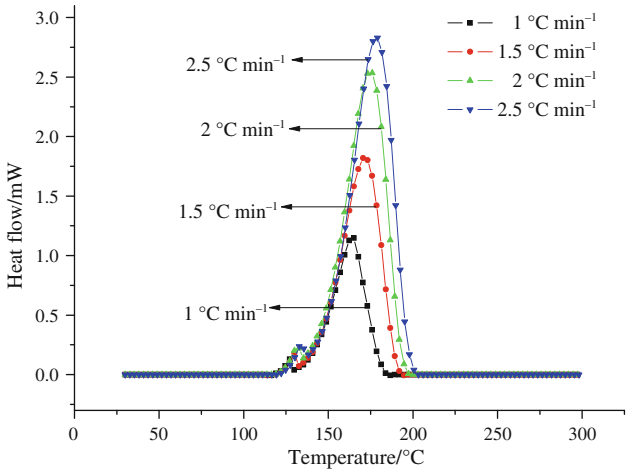

Fig. 5 DSC thermal curves of heat flow versus temperature for DTBP decomposition with scanning rates of 1, 1.5, 2, and 2.5 °C min^{-1}

parameters. In Figs. 4, 5, and 6, we also can see the greater the scanning rate the broader and smoother the thermal curve and unstable conversion rate of heat decomposition. Therefore, while analyzing CHP, DTBP, and TBPB thermokinetic parameters of thermal decomposition by non-isothermal kinetics, we propose a hypothetical statement, that from processing of model fitting or model free computed CHP, DTBP, and TBPB's thermokinetic parameters, we obtained a better result of scanning rates less than 2.5 °C min^{-1}.

Isothermal kinetic algorithm

Determination of thermokinetic parameters by TAM III

TAM III was employed to determine the thermokinetic and safety parameters of CHP, DTBP, and TBPB. Heat of

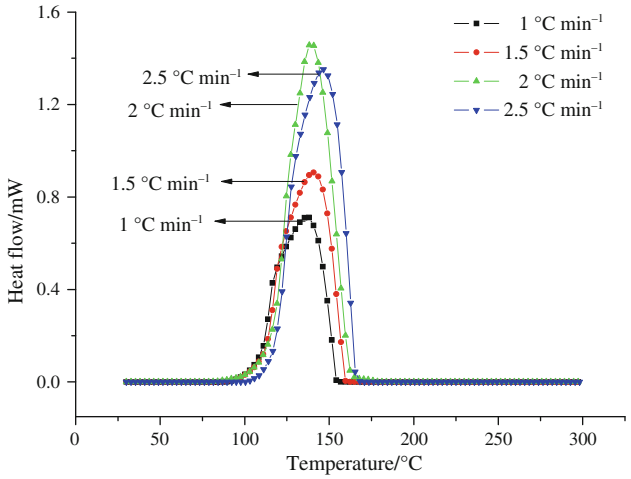

Fig. 6 DSC thermal curves of heat flow versus temperature for TBPB decomposition with scanning rates of 1, 1.5, 2, and 2.5 °C min^{-1}

Table 7 Results of CHP for scanning data of the thermal runaway decomposition via thermostat software by TAM III

Sample temperature/°C	TMR_{iso}/hour	Q/W g^{-1}	k_{iso}/min^{-1}	ΔH_d/J g^{-1}
80	141.7	0.00209	0.001104	1272.3
90	52.3	0.00277	0.002965	1283.2
100	38.4	0.00628	0.007967	2135.4
110	11.8	0.01799	0.019967	1238.4

Table 8 Results of DTBP for scanning data of the thermal runaway decomposition via Thermostat software by TAM III

Sample temperature/°C	TMR_{iso}/hour	Q/W g^{-1}	k_{iso}/min^{-1}	ΔH_d/J g^{-1}
80	30.8	0.00026	0.002375	788.3
90	21.1	0.00101	0.008861	775.4
100	11.3	0.00303	0.030809	803.9
110	0.6	0.01020	0.100376	897.1

decomposition and E_a were calculated at 80, 90, 100, and 110 °C isothermal temperatures. Tables 7, 8, and 9 show that while CHP, DTBP, and TBPB were operating under 80, 90, 100, and 110 °C, TMR_{iso} decreased and the highest heat flow increased as the isothermal temperature increased significantly. The hazard increased with lower E_a and TMR_{iso}. The highest heat flow could make the reaction become dangerous. Figures 7, 8, and 9 show the thermal curves of three liquid organic peroxides at four different isothermal temperatures, and indicate that when the temperature was increased from 80, 90, 100, and 110 °C the reaction time was correspondingly reduced.

Thermal curves by TAM III revealed that CHP, DTBP, and TBPB at the isothermal temperatures of 80, 90, 100, and

Table 9 Results of TBPB for scanning data of the thermal runaway decomposition via Thermostat software by TAM III

Sample temperature/°C	TMR_{iso}/hour	Q/W g^{-1}	k_{iso}/min^{-1}	ΔH_d/J g^{-1}
80	0.21	0.00333	0.004582	1208.6
90	0.19	0.01853	0.013590	991.2
100	0.15	0.04904	0.038024	1057.2
110	0.12	0.08993	0.100825	1046

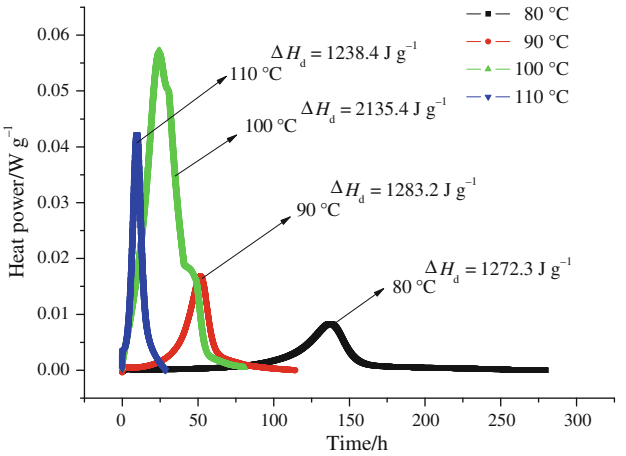

Fig. 7 TAM III thermal curves CHP decomposition with isothermal temperature at 80, 90, 100, and 110 °C

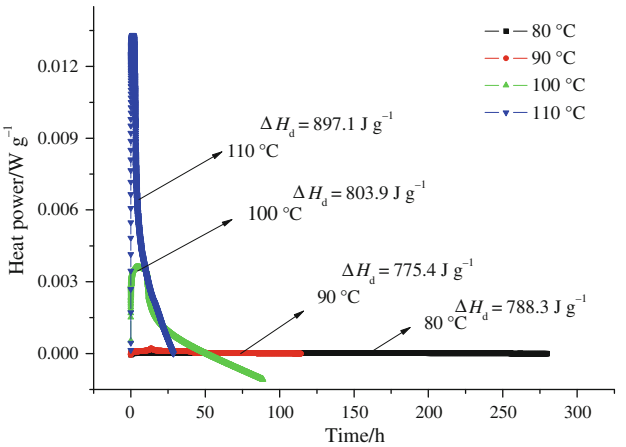

Fig. 8 TAM III thermal curves DTBP decomposition with isothermal temperature at 80, 90, 100, and 110 °C

110 °C followed mainly an nth order reaction and exhibited maximum heat flow values. By the Arrhenius equation

$$k_0 = A\exp\left(\frac{-E_a}{RT}\right) \tag{3}$$

where k_0 is the reaction rate constant; E_a is the activation energy of thermal decomposition; T is the absolute

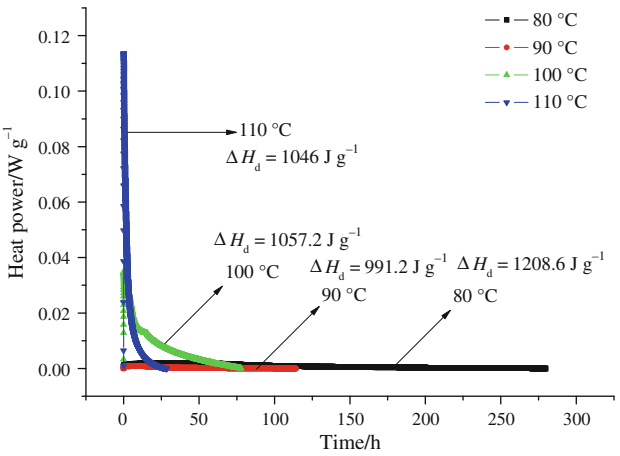

Fig. 9 TAM III thermal curves TBPB decomposition with isothermal temperature at 80, 90, 100, and 110 °C

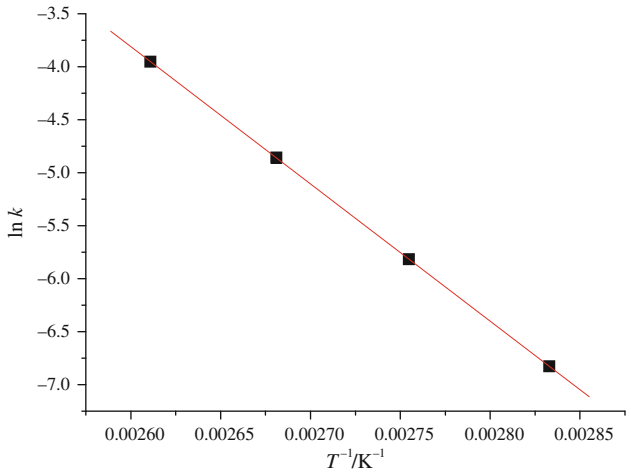

Fig. 10 CHP of activation energy analysis graph for Arrhenius plot at different isothermal temperatures at 80, 90, 100, and 110 °C

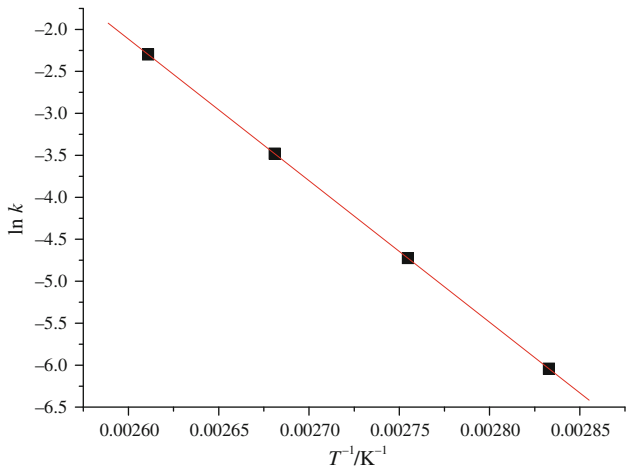

Fig. 11 DTBP of activation energy analysis graph for Arrhenius plot at different isothermal temperatures at 80, 90, 100, and 110 °C

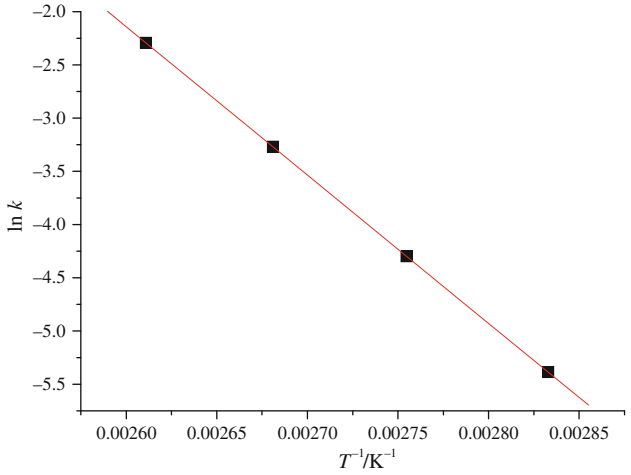

Fig. 12 TBPB of activation energy analysis graph for Arrhenius plot at different isothermal temperatures at 80, 90, 100, and 110 °C

temperature (K); R is the gas constant, and A is pre-exponential factor.

Equation (3) may be written in natural logarithm form:

$$\ln k_0 = \ln A - \frac{E_a}{RT_0} \tag{4}$$

Reaction rate constant k_0 increased with heat of decomposition. As the pre-exponential factor is constant, Eq. (4) could be expressed as a set of kinetic equations as follows:

$$\ln k_1 + \frac{E_a}{RT_1} = \ln k_2 + \frac{E_a}{RT_2} = \ln k_3 + \frac{E_a}{RT_3} = \ldots \tag{5}$$

where k_3 is the reaction rate constant of different isothermal temperatures; T_3 is the isothermal temperature. Tables 7, 8, and 9 show CHP, DTBP, and TBPB, that as the operating temperature increased from 80 to 110 °C, the reaction rate constant also increased. Raising the temperature makes the reaction rate constant faster. The values of ln$k$ versus T^{-1} are indicated in Figs. 10, 11, and 12. The Arrhenius plot gives a slope $= -E_a R^{-1}$. Hence, we could determine that the E_a of CHP, DTBP, and TBPB were 107.76, 117.28, and 115.82 kJ mol^{-1}, the correlation coefficients were 0.996, 0.994, and 0.997, and the ln$A$ were 29.89, 41.756, and 34.079, respectively.

Conclusions

We established an accurate analysis model on thermokinetic parameters of CHP, DTBP, and TBPB for non-isothermal and isothermal decomposition. In addition to realizing organic peroxide's thermal decomposition kinetic parameter analysis through DSC and TAM III approaches, we found that the DSC non-isothermal approach presented a reasonable mathematical model to match the TAM III isothermal approach for an organic peroxide's thermal decomposition E_a. Curve fitting had a decent reliability in analyzing E_a of CHP, DTBP, and TBPB for thermal decomposition. Furthermore, we obtained a fixed and simple mathematical model for the value retrieving range. We discovered a highly elaborate means to appraise the thermokinetic parameters for the three organic peroxides. To conduct the E_a of organic peroxide's thermal decomposition by non-isothermal approaches, we received better result that the scanning rates was lesser than 2.5 °C min^{-1}. Accordingly, this study established an effective and swift procedure for receiving information on thermal decomposition characteristics and reaction hazard of CHP, DTBP, and TBPB that could be employed as an intrinsically safer design during normal or upset operation.

Acknowledgements The authors are indebted to the donors of the National Science Council (NSC) in Taiwan under the contract number NSC-96-2625-Z-224-001 for financial support.

References

1. Huang D, Han M, Wang J, Jin Y. Catalytic decomposition process of cumene hydroperoxide using sulfonic resins as catalyst. Chem Eng J. 2002;88:215–23.
2. Hou HY, Shu CM, Tasi TL. Reactions of cumene hydroperoxide mixed with sodium hydroxide. J Hazard Mater. 2008;152:1214–9.
3. Lin DU, Xu YF, MaoFa GE, Jia L, Yao L. Experimental investigation of incremental reactivity of di-tert-butyl peroxide. Chin Sci Bull. 2007;52(12):1629–34.
4. Brandrup EJ, Immergut EH, Grulke EA. Polymer handbook, 4th ed. II/2-69; Aldrich Catalog No. Z41, John Wiley, New York, USA;1999. p. 247.
5. Lu Y, Ng D, Miao L, Mannan SM. Key observations of cumene hydroperoxide concentration on runaway reaction parameters. Thermochim Acta. 2010;501:65–71.
6. Material safety data sheet, Amersfoort, The Netherlands;2007.
7. Code for the storage of organic peroxide formulations, NFPA 432, National Fire Protection Association (NFPA), Quincy, MA, USA;2008.
8. STAR^e software with solaris operating system, operating instructions; Mettler Toledo, Sweden. 2004.
9. Ozawa T. A new method of analyzing thermogravimetric data. Bull Chem Soc. 1965;38:1881–6.
10. Flynn JH, Wall LA. Res Natl Bur Standards, Phys Chem. 1966;70:487–92.
11. Flynn JH, Wall LA. A quick, direct method for the determination of activation energy from thermogravimetric data. J Polym Sci. 1966;4:323–8.
12. Product Information, 2008, TAM III Thermostat. Available at: www.thermometric.com.
13. Cheng SY, Tseng JM, Lin SY, Gupta JP, Shu CM. Runaway reaction on tert-butyl peroxybenzoate by DSC tests. J Therm Anal Calorim. 2008;93:121–6.
14. Wu SH, Tsai TL, Hou HY, Tseng JM, Shu CM. 2006 Japan/Taiwan/Korea Chemical Engineering Conference, Japan 2006.

15. Chen CC, Shu CM, Yeh CA, Chen SC, Shu ML. The 17th Annual Conference of Asia Pacific occupational safety and health organization, Taipei, Taiwan, ROC 2001;295.
16. Ferguson HD, Towsend DI, Hofelich TC, Russel PM. Reactive chemicals hazard evaluation: Impact of thermal characteristics of transportation/storage vessels. J Hazard Mater. 1994;37:285–302.
17. Chen JR, Wu SH, Lin SY, Hou HY, Shu CM. Utilization of microcalorimetry for an assessment of the potential for a runaway decomposition of cumene hydroperoxide at low temperatures. J Therm Anal Calorim. 2008;93:127–33.
18. Lee RP, Hou HY, Tseng JM, Chang MK, Shu CM. Reactive incompatibility of DTBP mixed with two acid solutions. J Therm Anal Calorim. 2008;93:269–74.
19. The isothermal calorimetric manual for thermometric AB. Jarfalla, Sweden. 2007.
20. Hou HY, Shu CM, Duh YS. Exothermic decomposition of cumene hydroperoxide at low temperature conditions. AIChE J. 2001;47:1893–6.
21. You ML, Tseng JM, Liu MY, Shu CM. Runaway reaction of lauroyl peroxide with nitric acid by DSC. J Therm Anal Calorim. 2010;102:535–9.
22. Tseng JM, Liu MY, Chen SL, Hwang WT, Gupta JP, Shu CM. Runaway effects of nitric acid on methyl ethyl ketone peroxide by TAM III test. J Therm Anal Calorim. 2009;96:789–93.
23. Li XR, Koseki H. Thermal decomposition kinetic of liquid organic peroxides. J Loss Prev Process Ind. 2005;18:460–4.
24. Lin CP, Tseng JM, Chang YM, Liu SH, Cheng YC, Shu CM. Modeling liquid thermal explosion reactor containing tert-butyl peroxybenzoate. J Therm Anal Calorim. 2010;102:587–95.